arXiv:1510.09062v1 [quant-ph] 30 Oct 2015

Measurement of the squeezed vacuum state by a bichromatic local oscillator

Wei Li,[1,2], Xudong Yu,[1,2] and Jing Zhang[1,3,*]

[1] *The State Key Laboratory of Quantum Optics and Quantum Optics Devices, Institute of Opto-Electronics, Shanxi University, Taiyuan 030006, P.R.China*

[2] *Collaborative Innovation Center of Extreme Optics, Shanxi University, Taiyuan 030006, P.R.China*

[3] *Synergetic Innovation Center of Quantum Information and Quantum Physics, University of Science and Technology of China, Hefei, Anhui 230026, P. R. China*

[*] *Corresponding author: jzhang74@sxu.edu.cn, jzhang74@yahoo.com*

Compiled November 2, 2015

We present the experimental measurement of a squeezed vacuum state by means of a bichromatic local oscillator (BLO). A pair of local oscillators at ±5 MHz around the central frequency ω_0 of the fundamental field with equal power are generated by three acousto-optic modulators and phase-locked, which are used as a BLO. The squeezed vacuum light are detected by a phase-sensitive balanced-homodyne detection with a BLO. The baseband signal around ω_0 combined with a broad squeezed field can be detected with the sensitivity below the shot-noise limit, in which the baseband signal is shifted to the vicinity of 5 MHz (the half of the BLO separation). This work has the important applications in quantum state measurement and quantum information. © 2015 Optical Society of America

OCIS codes: (270.5585) Quantum information and processing; (270.6570) Squeezed states.

http://dx.doi.org/10.1364/OL.99.099999

Squeezed state of the light is an important resource of the quantum information [1–9] and quantum metrology [10–14]. Especially, in the modern research focus, the squeezed state becomes crucial for the gravitation wave detection. In recent years, some significant improvement have been made in this field, such as the 12.7 dB squeezing has been obtained [15], the very lower frequency squeezing measurement has been realized and the frequency-dependence squeezing has been investigated [16]. A single broadband squeezed light can be split into N pairs of upper and lower single sideband fields with spatial separation, which correspond to N independent EPR entangled fields [17]. This scheme was demonstrated experimentally by using a pair of frequency-shifted local oscillators to measure this EPR entanglement [18,19]. The theoretical scheme based on a bichromatic local oscillator (BLO) to detect the squeezed state was proposed [20], in which several advantages and applications were given. The phase-sensitive detection with a BLO or a double-sideband signal field were studied [21–23]. In this paper, we utilize a BLO to detect a broadband squeezed light with a phase-sensitive balanced-homodyne detection. This work demonstrates quantum correlation between the upper and lower sideband modes [17] of a single broadband squeezed light from another perspective. Generating and measuring the low frequency squeezing for the terrestrial gravitational wave detectors are very tough because of the extremely challenges in the technique. The BLO technique can circumvent the challenge of detecting low frequency squeezing, which is usually obscured by technical noise. We present the result that the baseband signal is shifted into the vicinity of 5 MHz ((the half of the BLO separation) and sub-shot-noise detection is implemented. Thus this work with the BLO and broadband squeezing can be used to enhance the signal-to-noise ratio (SNR) of an interferometer for lower frequency phase measurement [24, 25].

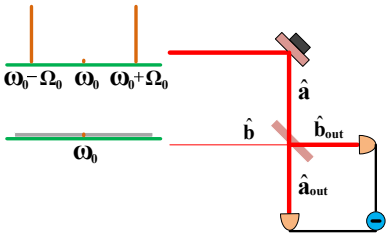

Fig. 1. The schematic diagram of measuring a single broadband squeezed light with the central frequency ω_0 using a phase-sensitive balanced-homodyne detection with a BLO.

The schematic diagram of the detection is shown in Fig. 1. A strong BLO (at $\pm\Omega_0$ around the central frequency ω_0 of the fundamental field with equal power) is mixed with the signal light field at a 50/50 beam splitter. The relative phase θ of the local oscillator and the signal field can be controlled by the reflective mirror mounted on a PZT (piezoelectric transducer). The annihilation operators of the bichromatic local oscillator and the signal field can be written as $\hat{a}(t) = \hat{a}_+(t)\exp[-i(\omega_0+\Omega_0)t] + \hat{a}_-(t)\exp[-i(\omega_0-\Omega_0)t]$ and $\hat{b}(t) = \hat{b}_0(t)\exp(-i\omega_0 t)$, where $\hat{a}_{+(-)}(t)$ and $\hat{b}_0(t)$ are the slow varying operators of the fields. The output

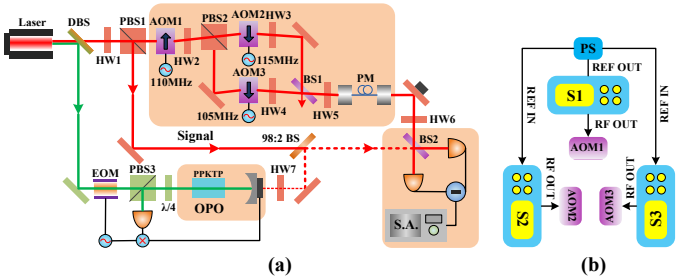

Fig. 2. (a) The setup for the experimental realization of measuring vacuum squeezing by a phase-sensitive balanced-homodyne detection with a bichromatic local oscillator. DBS1,2: dichroic beam splitter; HW1-4: half wave plate; BS1,2: 50/50 beam splitter; AOM1-3: acousto-optic modulator; PM: single-mode polarization-maintaining optical fiber. EOM: electro-optical modulator. OPO: optical parametric oscillator. SA: spectrum analyzer. (b) The scheme for locking the relative frequency and phase of the double sidebands. PS: power splitter for radio frequency.

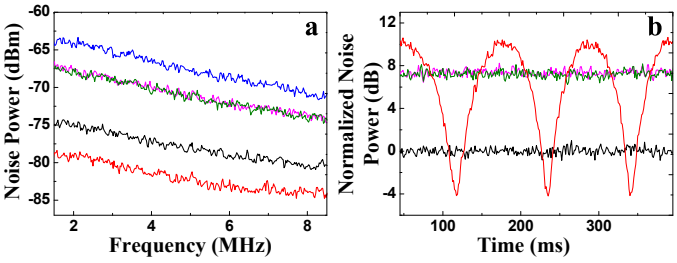

Fig. 3. The measured noise power spectra. (a) The noise power spectra at the analysis frequencies from 1.5 MHz to 8.5 MHz with the resolution bandwidth of 100 kHz and the video bandwidth of 300 Hz. The blue line: the anti-squeezing component; The red line: the squeezing component; (b): The noise power spectra at the analysis frequency of 5 MHz are measured by scanning the relative phase of θ. The red line: the quadrature component; The black line: shot noise limit; The green and pink lines: the noise power spectrum when the single sideband of the bichromatic local oscillator is used respectively. Here, the electric (dark) noise is about 14 dB below SNL.

fields of the 50/50 beam splitter are

$$\hat{a}_{out}(t) = [\hat{a}(t)e^{i\theta} + \hat{b}(t)]/\sqrt{2}, \quad (1)$$
$$\hat{b}_{out}(t) = [\hat{a}(t)e^{i\theta} - \hat{b}(t)]/\sqrt{2}. \quad (2)$$

Therefore, the normalized difference of the photocurrents of the two detectors may be

$$\hat{i}(t) = \frac{1}{\sqrt{2}a}[\langle\hat{a}^\dagger(t)\rangle\hat{b}(t)e^{-i\theta} + \langle\hat{a}(t)\rangle\hat{b}^\dagger(t)e^{i\theta}], \quad (3)$$

where the fields satisfy $\langle\hat{a}_+\rangle = \langle\hat{a}_-\rangle = a \gg \langle\hat{b}_0\rangle \sim 0$. Therefore the signal field may be the vacuum state or the squeezed vacuum state. And the bichromatic local oscillator is a pair of the strong and equal coherent states.

The difference of the photocurrents analyzed at the radio frequency Ω is expressed as

$$\hat{i}(\Omega) = \frac{1}{\sqrt{2}}[\hat{b}(\Omega_0-\Omega)+\hat{b}(-\Omega_0-\Omega)]e^{-i\theta} + \frac{1}{\sqrt{2}}[\hat{b}^\dagger(\Omega_0+\Omega)+\hat{b}^\dagger(-\Omega_0+\Omega)]e^{i\theta}. \quad (4)$$

Here, we express the quadrature component of the signal field around the central frequency ω_0, which easily compare with the measurement with a single local oscillator at ω_0. Therefore, the quadrature component of the signal field can be defined as $\hat{Q}_S(\nu,\theta) = \hat{b}(-\nu)e^{-i\theta} + \hat{b}^\dagger(\nu)e^{i\theta}$ at the analysis frequency ν, which includes the up and down sideband modes $\pm\nu$. The quadrature amplitude ($\theta = 0$) can be $\hat{X}_S(\nu) = \hat{b}(-\nu) + \hat{b}^\dagger(\nu)$ and the quadrature phase ($\theta = \pi/2$) $\hat{Y}_S(\nu) = -i[\hat{b}(-\nu) - \hat{b}^\dagger(\nu)]$. The difference of the photocurrents with the bichromatic local oscillator (Eq. 4) will give the information of the quadrature component of the signal field

$$\hat{Q}_B(\Omega,\theta) = \frac{1}{\sqrt{2}}[\hat{Q}_S(|\Omega_0-\Omega|,\theta) + \hat{Q}_S(\Omega_0+\Omega,\theta)] \quad (5)$$

Here, Ω is the analysis frequency of the bichromatic local oscillator detection. We can know from here that there are two pairs of the sideband modes $\pm|\Omega_0-\Omega|$ and $\pm(\Omega_0+\Omega)$ to be measured by the bichromatic local oscillator. The arbitrary quadrature component of the signal field can be measured by scanning the relative phase of θ. So when $\theta = 0$, the difference of the photocurrents will give the information of the quadrature amplitude of the signal field $\hat{X}_B(\Omega) = \frac{1}{\sqrt{2}}[\hat{X}_S(|\Omega_0-\Omega|) + \hat{X}_S(\Omega_0+\Omega)]$, and when $\theta = \pi/2$, the quadrature phase $\hat{Y}_B(\Omega) = \frac{1}{\sqrt{2}}[\hat{Y}_S(|\Omega_0-\Omega|) + \hat{Y}_S(\Omega_0+\Omega)]$.

For the broad quadrature phase squeezing as the input signal field, the quadrature components satisfy $\langle\Delta^2\hat{Y}_S(|\Omega_0-\Omega|)\rangle = \langle\Delta^2\hat{Y}_S(\Omega_0+\Omega)\rangle = e^{-2r} < 1$ and $\langle\Delta^2\hat{X}_S(|\Omega_0-\Omega|)\rangle = \langle\Delta^2\hat{X}_S(\Omega_0+\Omega)\rangle = e^{2r} > 1$, where r is the squeezing parameter. Correspondingly, we can obtain the variance of the quadrature components of the signal field by means of a bichromatic local oscillator,

$$\langle\Delta^2\hat{Y}_B(\Omega)\rangle = e^{-2r} < 1, \langle\Delta^2\hat{X}_B(\Omega)\rangle = e^{2r} > 1. \quad (6)$$

So the difference of the output photocurrents at the analyzed frequency Ω presents quadrature phase squeezing of the two pairs of the sideband modes $\pm|\Omega_0-\Omega|$ and $\pm(\Omega_0+\Omega)$. Thus, when the squeezing spectrum of the input field can reach the frequency of $2\Omega_0$, we may obtain the baseband signal around ω_0 of the input field below the shot-noise limit at the analyzed frequency Ω_0 of the measured noise spectrum.

Figure 2 shows the experimental setup. The laser source, which is a diode-pumped external-cavity frequency doubled laser, provides the second-harmonic light of 450 mW at 532 nm and the fundamental light of 200 mW at 1064 nm simultaneously. The second harmonic

light is used to pump the OPO (optical parametric oscillator). The fundamental light is separated into two parts. One is utilized as the auxiliary beam to adjust the interference of the local oscillator and the detected field. The other is used to generate the bichromatic local oscillator by three acousto-optic modulators and phase-locked technology. The frequency shifts of AOM1, AOM2 and AOM3 are +110 MHz, -115 MHz and -105 MHz respectively. The two frequency-shifted laser beams at $\omega_0 \pm \Omega_0$ ($\Omega_0 = 5$ MHz) are combined on 50% BS1 with the same polarization. The bichromatic laser field is coupled into a single-mode polarization-maintaining fiber to filter the spatial modes. As above discussion, only when the up- and down-shifted frequencies (Ω_+ and Ω_-) around the central frequency ω_0 of the bichromatic local oscillator are same ($\Omega_+ = \Omega_- = \Omega_0$) and the relative phase is fixed, the measurement for the broad squeezed light becomes the balanced homodyne detection. The two methods of locking the relative phase between up- and down-shifted laser fields have been developed in our previous work [22]. Here we employ the clock synchronization of the signal generators. The three signal generators for driving the AOMs can be locked together in frequency and phase by using the same reference (clock) frequency.

The resonator for the squeezed light is a semi-monolithic triple-resonant OPO. The cavity is 38 mm long, and consists of a 10 mm long PPKTP crystal. The front facet of crystal acts as the input coupler, has a transmittance of 5 % for 532 nm and is highly reflective for 1064 nm. The rear facet is anti-reflective for both 532 nm and 1064 nm. The output mirror of the OPO has a transmittance of 12.5 % for 1064 nm and is highly reflective for 532 nm. The cavity bandwidth is around 70 MHz. The PPKTP is a type I quasi-phase-matching crystal and its phase-matching condition is achieved by the temperature controller [26, 27]. The OPO cavity is locked according to the PDH technique, the error signal is derived from the reflected pump field. By adjusting the reflective mirror of LO mounted on PZT, the relative phase θ between the bichromatic LO and the squeezed light field is changed. The squeezed state is mixed with the bichromatic local oscillator on the 50/50 beam splitter with the interference fringe visibility of 98 %. At last the two output fields of the beam splitter are measured by two balanced detectors.

Fig. 3 shows the noise power spectra measured by means of a bichromatic local oscillator. The power of the pump field of the OPO is about 40 mW. The total power of the bichromatic local oscillator is set 4.0 mW. In the analysis frequency regime from 1.5 MHz to 8.5 MHz, the squeezing value is 4.1 ± 0.2 dB ($\langle \Delta^2 \hat{Y} \rangle = 0.39 \pm 0.02$), and the anti-squeezing is about 10.1 ± 0.2 dB ($\langle \Delta^2 \hat{X} \rangle = 10.2 \pm 0.5$) higher than SNL (Fig. 3(a)). The noise power spectra at the analysis frequency of 5 MHz with zero span are measured by scanning the relative phase of θ (Fig. 3(b)). It demonstrates that the bichromatic local oscillator is a phase-sensitive balanced-homodyne detection and the arbitrary quadrature components can be measured (the red line in Fig. 3(b)). When one of the bichromatic local oscillator is blocked to become a single local oscillator, the detection is changed into the heterodyne detection and the noise spectrum is 7.3 ± 0.2 dB higher than the SNL, which is insensitive to the relative phase of θ (The green and pink lines in Fig. 3). It is consistent well with the estimation 7.25 dB ($(\langle \Delta^2 \hat{Y} \rangle + \langle \Delta^2 \hat{X} \rangle)/2 = 5.3$) according to the above measurements.

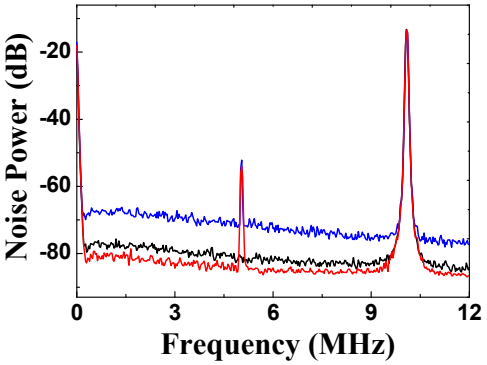

Fig. 4. The noise spectra at analysis frequency from 0 MHz to 12 MHz with a baseband signal field around ω_0. The red line: the baseband signal peak at 5 MHz with the squeezed quadrature component; The blue line: the baseband signal peak with the antisqueezed quadrature component. The black line: shot noise limit. The peak at 10 MHz is due to the beatnote of the bichromatic local oscillator. Here, the electric (dark) noise is about 14 dB below SNL. The power of the LO and the signal is 4 mW and about 200 nW respectively. RBW = 30 kHz, VBW = 1 kHz, Sweep time=200 ms.

When a baseband signal field around ω_0 is added into the squeezed vacuum field by a 98/2 beam splitter, the noise spectra at analysis frequency from 0 MHz to 12 MHz is given in Fig. 4 by means of the bichromatic local oscillator detection. The baseband signal peak appears at 5 MHz, whose sensitivity is 4.1 dB below the shot-noise limit when the squeezed quadrature component is detected (the red line in Fig. 4). It demonstrates that the baseband signal is shifted into the vicinity of 5 MHz ((the half of the BLO separation) and sub-shot-noise detection is obtained.

In conclusion, we study a phase-sensitive balanced-homodyne detection with a bichromatic local oscillator. The baseband signal field around ω_0 with a broad squeezed field is detected and the sensitivity of the signal can be below the shot-noise limit. This detection scheme can be employed in gravitational-wave detection and the quantum information process.

We acknowledge the financial support from the National Basic Research Program of China (Grant No. 2011CB921601), National Natural Science Foundation of China (NSFC) (Grant No. 11234008, 11361161002, 61571276), Natural Science Foundation of Shanxi

Province (Grant No. 2015011007).

References

1. A. Furusawa, J. L. Sørensen, S. L. Braunstein, C. A. Fuchs, H. J. Kimble, and E. S. Polzik, Science **282**, 706 (1998).
2. W. P. Bowen, N. Treps, B. C. Buchler, R. Schnabel, T. C. Ralph, H. -A. Bachor, T. Symul, and P. K. Lam, Phys. Rev. A **67**, 032302 (2003).
3. X. Li, Q. Pan, J. Jing, J. Zhang, C. Xie, and K. Peng, Phys. Rev. Lett. **88**, 047904 (2002).
4. R. Ukai, N. Iwata, Y. Shimokawa, S. C. Armstrong, A. Politi, J. Yoshikawa, P. van Loock, and A. Furusawa, Phys. Rev. Lett. **106**, 240504 (2011).
5. X. Jia, J. Zhang, Y. Wang, Y. Zhao, C. Xie, and K. Peng, Phys. Rev. Lett. **108**, 190501 (2012).
6. X. Su, S. Hao, X. Deng, L. Ma, M. Wang, X. Jia, C. Xie, and K. Peng, Nature Commun. **4**, 2828 (2013).
7. K. Liu, J. Guo, C. Cai, S. Guo, and J. Gao, Phys. Rev. Lett. **113**, 170501 (2014).
8. S. L. Braunstein, and P. van Loock, Rev. Mod. Phys. **77**, 513 (2005).
9. C. Weedbrook, S. Pirandola, R. García-Patrón, N. J. Cerf, T. C. Ralph, J. H. Shapiro, and S. Lloyd, Rev. Mod. Phys. **84**, 621 (2012).
10. R. Schnabel, N. Mavalvala, D. E. McClelland, and P. K. Lam, Nature Commun. **1**, 121 (2010).
11. V. Giovannetti, S. Lloyd, and L. Maccone, Nature Photonics **5**, 222 (2011).
12. S. Steinlechner, J. Bauchrowitz, M. Meinders, H. M. Ebhardt, K. Danzmann, and R. Schnabel, Nature Photonics **7**, 626 (2013).
13. V. Giovannetti, S. Lloyd, and L. Maccone, Phys. Rev. Lett. **96**, 010401 (2006).
14. H. Yonezawa, D. Nakane, T. A. Wheatley, K. Iwasawa, S. Takeda, H. Arao, K. Ohki, K. Tsumura, D. W. Berry, T. C. Ralph, H. M. Wiseman, E. H. Huntington, and A. Furusawa, Science **337**, 1514 (2012).
15. T. Eberle, S. Steinlechner, J. Bauchrowitz, V. Händchen, H. Vahlbruch, M. Mehmet, H. M. Ebhardt, and R. Schnabel, Phys. Rev. Lett **104**, 251102 (2010).
16. S. Chelkowski, H. Vahlbruch, B. Hage, A. Franzen, N. Lastzka, K. Danzmann, and R. Schnabel, Phys. Rev. A **71**, 013806 (2005).
17. J. Zhang, Phys. Rev. A **67**, 054302 (2003).
18. E. H. Huntington, G. N. Milford, C. Robilliard, T. C. Ralph, O. Glökl, U. L. Andersen, S. Lorenz, and G. Leuchs, Phys. Rev. A **71**, 041802 (2005).
19. B. Hage, A. Samblowski, and R. Schnabel, Phys. Rev. A **81**, 062301 (2010).
20. A. M. Marino, C. R. Stroud, J. V. Wang, R. S. Bennink, and R. W. Boyd, J. Opt. Soc. Am. B **24**, 335 (2007).
21. H. Fan, D. He, and S. Feng, arXiv:1410.8602.
22. W. Li, X. Yu, Z. Meng, Y. Jin and J. Zhang, Sci. China-Phys. Mech. Astron. **58**, 104201 (2015); arXiv:1508.04974 (2015).
23. J. -B. Béguin, E. M. Bookjans, S. L. Christensen, H. L. Sørensen, J. H. Müller, E. S. Polzik, and J. Appel, Phy. Rev. Lett. **113**, 263603 (2014).
24. B. Yurke, P. Grangier, and R. E. Slusher, J. Opt. Soc. Am. B **4**, 1677 (1987).
25. Z. Zhai, and J. Gao, Opt. Express **20**, 18173 (2012).
26. J. Zhang, C. Ye, F. Gao, and M. Xiao, Phys. Rev. Lett. **101**, 233602 (2008).
27. K. Di, X. Yu, and J. Zhang, Acta Sin. Quantum Opt. **16**, 241 (2010).